Catalytic Cycle of ATP Hydrolysis by P-Glycoprotein: Evidence for Formation of the E·S Reaction Intermediate with ATP-γ-S, a Nonhydrolyzable Analogue of ATP†

Zuben E. Sauna,‡ In-Wha Kim,‡ Krishnamachary Nandigama,‡ Stephan Kopp,§ Peter Chiba,§ and Suresh V. Ambudkar*,‡

Laboratory of Cell Biology, Center for Cancer Research, National Cancer Institute, National Institutes of Health, Bethesda, Maryland 20892-4256, and Institute of Medicinal Chemistry, Medical University of Vienna, Waehringerstrasse 10, Vienna, A-1090 Austria

Received July 13, 2007; Revised Manuscript Received September 17, 2007

ABSTRACT: Structural and biochemical studies of ATP-binding cassette (ABC) transporters suggest that an ATP-driven dimerization of the nucleotide-binding domains (NBDs) is an important reaction intermediate of the transport cycle. Moreover, an asymmetric occlusion of ATP at one of the two ATP sites of P-glycoprotein (Pgp) may follow the formation of the symmetric dimer. It has also been postulated that ADP drives the dissociation of the dimer. In this study, we show that the E·S conformation of Pgp (previously demonstrated in the E556Q/E1201Q mutant Pgp) can be obtained with the wild-type protein by use of the nonhydrolyzable ATP analogue ATP-γ-S. ATP-γ-S is occluded into the Pgp NBDs at 34 °C but not at 4 °C, whereas ATP is not occluded at either temperature. Using purified Pgp incorporated into proteoliposomes and ATP-γ-^{35}S, we demonstrate that the occlusion of ATP-γ-^{35}S has an E_{act} of 60 kJ/mol and the stoichiometry of ATP-γ-^{35}S:Pgp is 1:1 (mol/mol). Additionally, in the conserved Walker B mutant (E556Q/E1201Q) of Pgp, we find occlusion of the nucleoside triphosphate but not the nucleoside diphosphate. Furthermore, Pgp in the occluded nucleotide conformation has reduced affinity for transport substrates. These data provide evidence for the ATP-driven dimerization and ADP-driven dissociation of the NBDs, and although two ATP molecules may initiate dimerization, only one is driven to an occluded pre-hydrolysis intermediate state. Thus, in a full-length ABC transporter like Pgp, it is unlikely that there is complete association and disassociation of NBDs and the occluded nucleotide conformation at one of the NBDs provides the power-stroke at the transport−substrate site.

The ATP-binding cassette (ABC)[1] family represents one of the largest and most diverse families of transport proteins (*1*). There are 48 human ABC proteins, of which 17 are implicated in diseases (*2*). P-glycoprotein (Pgp, ABCB1) was the first eukaryotic ABC transporter identified and is clinically important because of its role in conferring multidrug resistance (MDR) to cancer cells (*3*). Pgp consists of two nucleotide-binding domains (NBDs) and two transmembrane domains (TMDs). The NBDs show extensive amino acid sequence identity and contain the conserved motifs Walker A, Walker B, A-, Q-, H-, and D-loops and the signature sequence (*4*). The TMDs, on the other hand, show little sequence homology. Each TMD typically consists of six transmembrane helices, and both TMDs participate in the formation of overlapping, multiple substrate-binding sites. Transport by ABC proteins involves conformational changes in the TMDs that convert a high-affinity drug-substrate site that is inward-facing (accessible from the cell interior) to a low-affinity site that is outward-facing (*5*). These conformational changes are coupled to ATP-binding and hydrolysis. Early models to explain the transport mechanism of Pgp have evolved to incorporate new concepts that have come from structural and biochemical studies of bacterial ABC proteins, and there has also been an effort to synthesize generalized models of transport (*6*).

The essential feature of the nucleotide binding pocket is that the ATP is sandwiched between the Walker A, Walker B, Q-, and H-loops of one NBD and the D-loop and signature sequence of the apposing NBD; hence the term ATP sandwich. Such an architecture was predicted by the modeling studies of Jones and George (*7*) based on the first high-resolution structure of an ABC subunit, HisP (*8*). Biochemical studies with MJ0796 demonstrated the ATP-driven dimerization of the NBDs by use of the E171Q mutant, which binds but does not hydrolyze ATP (*9*). This mutant was subsequently used to determine the structure of a NBD dimer with bound ATP at the interface (*10*). Furthermore, structures of MalK (the NBD submit of the *Escherichia coli* maltose transporter) have been obtained in open, semi-open, and closed conformations, where the closed conformation is a dimer with two ATPs bound at the interface (*11*). More recently, both biochemical (*12*) and structural studies (*13*)

† This work was supported by the Intramural Research Program, Center for Cancer Research, National Cancer Institute, NIH.

* Address correspondence to this author: phone 301-402-4178; fax 301-435-8188; e-mail ambudkar@helix.nih.gov.

‡ National Institutes of Health.

§ Medical University of Vienna.

[1] Abbreviations: ABC, ATP-binding cassette; BeF_x, beryllium fluoride; AMPPNP, adenyl-5′-yl imidodiphosphate; AMPPCP, 5′-adenylylmethylenediphosphate; [^{125}I]IAAP, [^{125}I]iodoarylazidoprazosin; NBD, nucleotide binding domain; Pgp, P-glycoprotein; PAGE, polyacrylamide gel electrophoresis; PEI, poly(ethylenimine); PP_i, sodium pyrophosphate; TLC, thin-layer chromatography; Vi, orthovanadate.

10.1021/bi701385t CCC: $37.00
Published on Web 11/08/2007

have demonstrated a ATP-driven dimerization in the isolated NBDs of the *E. coli* hemolysin transporter, HlyB. An important concept has emerged from these studies: the ATP-driven dimerization of NBDs. The isolated NBDs of ABC proteins exist as monomers and the ATP sites show an open conformation in the absence of nucleotide. The addition of nucleotide induces dimerization of the NBDs in the head-to-tail configuration described above. The nucleotide occupies a significant part of the dimer interface and stabilizes the dimeric state by altering the electrostatic charge balance (*10*). This closure is driven primarily by interactions between the γ-phosphate and the signature motif (*14*), a fact consistent with biochemical evidence that shows that ADP cannot induce dimerization (*9*, *15*). ATP-driven dimerization has an activation energy of 60−70 kJ/mol (*16*, *17*), which suggests relatively large conformational changes (*18*). In addition, the fact that dimerization is temperature-dependent poses a technical problem because ATP would be hydrolyzed to ADP, which does not permit formation of the nucleotide sandwich. One strategy to obtain a stable ATP-driven dimer has been to mutate a highly conserved glutamate in the Walker B domain of ABC proteins (E556 and E1201 in human Pgp). These mutants bind ATP with normal kinetics (*16*, *19*) but ATP hydrolysis is severely impaired (>95%). In bacterial ABC proteins, such mutants exhibit ATP-driven dimerization (*9*, *10*, *17*). The E556Q/E1201Q and the E552A/E1197A double mutants of human and mouse Pgps, respectively, have been extensively characterized in recent years (*16*, *19*−*22*). These double mutants of Pgp occlude nucleotide (predominantly as the nucleoside triphosphate) in a tightly bound nonexchangeable form in the absence of Vi or beryllium fluoride (BeF_x). This reaction intermediate has been alluded to as the "occluded nucleotide conformation" (*22*). Unlike the ATP-driven dimers obtained with isolated NBDs, which exhibit a stoichiometry of 2 mol of ATP/dimer (*10*, *15*), the occluded nucleotide conformation of Pgp shows a maximal stoichiometry of 1 mol of ATP occluded/mol of Pgp (*16*, *21*). This has led to the suggestion that the ATP-bound state and the occluded nucleotide state may not be the same.

The distinction between a nucleotide-bound and occluded state is an important one, and it has been suggested that there are three distinct states of Pgp leading up to the occluded conformation (*22*). The first is an open dimer, the second is a symmetric closed dimer with ATPs bound at both NBDs, and the third is an asymmetric occluded state where one of the two ATPs is tightly bound in a nonexchangeable form (see refs *22* and *23* for reviews that discuss the experimental evidence). The postulate that an asymmetric occluded nucleotide conformation is a reaction intermediate of the catalytic cycle also impinges on the models used to describe the mechanism of ATP hydrolysis by ABC transporters. The alternating catalytic site model propounded by Senior et al. (*24*) postulated that only one of the two ATP sites hydrolyzes ATP at any given time and that catalysis at the two sites alternates. In recent years, a processive clamp model has been proposed (*15*, *17*) where ATP binding to two monomeric NBDs leads to formation of a dimer that, following hydrolysis of both NBDs, dissociates and releases ADP. In the latter model there is no distinction between the symmetric dimerization and asymmetric occlusion.

In this study, we compared the affinities of the nonhydrolyzable ATP analogues AMPPNP and ATP-γ-S for Pgp. As AMPPNP had a very low affinity for Pgp, we used ATP-γ-S to characterize nucleotide-driven dimerization. In addition, several other nonhydrolyzable analogues of ATP, such as AMPPCP, are not recognized by the NBDs of Pgp. We demonstrate temperature-dependent occlusion of ATP-γ-^{35}S in wild-type Pgp with a stoichiometry of 1 mol of ATP-γ-^{35}S/mol of Pgp. We also show that the occluded nucleotide conformation of Pgp shows reduced binding of the photoaffinity transport substrate [^{125}I]iodoarylazidoprazosin ([^{125}I]-IAAP) as well as reduced affinity for the propafenone GPV51. The kinetics and thermodynamics of ATP-γ-S occlusion in wild-type Pgp are comparable to those for the occlusion of ATP in the mutant (E556Q/Q1201Q) Pgp, described previously (*16*). Finally, we show, using the Walker B glutamate (E556Q/E1201Q) mutant of Pgp, that the occluded nucleotide conformation could be generated with 8-azido-[α-^{32}P]ATP but not 8-azido-[α-^{32}P]ADP, which supports the hypothesis that the γ-phosphate plays a critical role in driving the closure of the NBDs (*14*). Our results suggest that ATP-driven dimerization of nucleotide binding domains, asymmetric occlusion of one nucleotide, and ADP-driven disassembly of the occluded state are important and distinct reaction intermediates of the Pgp transport cycle. Our findings also demonstrate that ATP-γ-S, the nonhydrolyzable analogue of ATP, may be useful to generate pre-hydrolysis [E·S] intermediate in other ABC transporters.

EXPERIMENTAL PROCEDURES

Chemicals. [^{125}I]Iodoarylazidoprazosin ([^{125}I]-IAAP), 2200 Ci/mmol; [α-^{32}P]ATP, 3000 Ci/mmol; and ATP-γ-^{35}S were obtained from Perkin-Elmer Life Sciences (Boston, MA). 8-Azido-[α-^{32}P]ATP (15−20 Ci/mmol), 8-azido-[α-^{32}P]ADP, (15−20 Ci/mmol), 8-azido-ATP, and 8-azido-ADP were purchased from Affinity Labeling Technologies, Inc. (Lexington, KY). The Pgp-specific monoclonal antibody C-219 was obtained from Fujirebio Diagnostics Inc. (Malvern, PA). All other chemicals were obtained from Sigma Chemical Co. (St. Louis, MO).

Preparation of Crude Membranes from High Five Insect Cells Infected with Recombinant Baculovirus Carrying the Wild-Type and Mutant Human MDR1 Gene. HighFive insect cells (Invitrogen, Carlsbad, CA) were infected with the recombinant baculovirus carrying the human *MDR1* cDNA (either wild-type or the mutant, E556/1201Q) with a 6× histidine tag at the C-terminal end as described (*25*). Crude membranes were prepared as described previously (*25*, *26*).

Purification and Reconstitution of Pgp. Human Pgp from crude membranes of High Five insect cells was purified as described previously (*27*). The crude membranes were solubilized with octyl β-D-glucopyranoside (1.25%) in the presence of 20% glycerol and a lipid mixture (0.1%). Solubilized proteins were subjected to metal affinity chromatography (Talon resin, Clontech, Palo Alto, CA) in the presence of 1.25% octyl β-D-glucopyranoside and 0.01% lipid; >90% purified Pgp was eluted with 200 mM imidazole at pH 6.8. Pgp in the 200 mM imidazole fraction was then concentrated (Centriprep-50, Amicon, Beverly, MA) to ~1.5−2.0 mg/mL and stored at −70 °C. Pgp was identified by immunoblot analysis using the monoclonal antibody C219

and quantified by the Schaffner and Weissmann protein estimation method (*34*) as previously described (*27*). Purified Pgp was reconstituted into proteoliposomes by dialysis with a lipid:protein ratio (w/w) of 6:1 as described (*16*, *28*). The orientation of Pgp in the proteoliposomes and specific activity of purified Pgp have been discussed previously (*16*).

Photo-cross-linking of 8-Azido-[α-^{32}P]ATP or 8-Azido-[α-^{32}P ADP to Pgp. Crude membranes of High Five insect cells (50−100 μg of protein) or purified and reconstituted protein (5−10 μg of protein) were incubated in the ATPase assay buffer (50 mM MES-Tris, pH 6.8, 50 mM KCl, 5 mM sodium azide, 2 mM EGTA, 2 mM dithiothreitol, 1 mM ouabain, and 10 mM $MgCl_2$) containing 10 μM 8-azido-[α-^{32}P]ATP (10 μCi/nmol) in the dark at 4 °C for 5 min. The samples were irradiated with a UV lamp assembly (PGC Scientifics, Gaithersburg, MD) fitted with two black-light (self-filtering) UV-A long wave F15T8BLB tubes (365 nm) for 10 min on ice (4 °C). Ice-cold ATP (10 mM) was added to displace excess noncovalently bound 8-azido-[α-^{32}P]ATP. After SDS−PAGE on a 7% NuPAGE gel, the gels were dried and exposed to Bio-Max MR film (Eastman Kodak Co.) at −70 °C for 12−24 h. The radioactivity incorporated into the Pgp band was quantified by use of the STORM 860 PhosphorImager system (Molecular Dynamics, Sunnyvale, CA) and the software ImageQuaNT.

Vanadate- or Beryllium Fluoride-Induced Trapping of Nucleotide into Pgp. The Pgp•8-azido-ADP•Vi/BeF_x reaction intermediates were generated as described previously (*16*, *29*). Crude membranes of High Five insect cells (100 μg) or purified and reconstituted protein (5−10 μg) were incubated in the ATP assay buffer (see above) containing 50 μM 8-azido-[α-^{32}P]ATP or 8-azido-[α-^{32}P]ADP (5 μCi/nmol) and 300 μM Vi or 0.2 mM $BeSO_4$ + 2.5 mM NaF in the dark at 34 °C for 5 min. The reaction was stopped by the addition of 10 mM ice-cold ATP, and the samples were placed immediately on ice. The samples were photo-cross-linked and electrophoresed, and the radioactivity incorporated in the Pgp band quantified as described (*29*).

Trapping of 8-Azido-[α-^{32}P]ATP into Mutant (E556Q/E1201Q) Pgp. Crude membranes of High Five insect cells (100 μg) or purified and reconstituted protein (5−10 μg) were incubated in the ATP assay buffer (see above) containing 50 μM 8-azido-[α-^{32}P]ATP (5 μCi/nmol) in the dark at 34 °C for 5 min. The reaction was stopped by the addition of 10 mM ice-cold ATP and placing the samples immediately on ice. The samples were photo-cross-linked and electrophoresed, and the radioactivity incorporated in the Pgp band was quantified as described (*16*).

ATPase Assays. ATPase activity of Pgp in crude membranes was measured by the end-point P_i assay as previously described (*30*, *31*), with minor modifications. Pgp-specific activity was recorded as the Vi-sensitive ATPase activity. The assay measured the amount of inorganic phosphate released over 20 min at 34 °C in the ATPase assay buffer. ATPase assays of Pgp are usually carried out at 37 °C. However, we found in a previous study that occlusion of ATP in the E556Q/E1201Q mutant Pgp is maximal between 30 and 34 °C, and there is a substantial (∼20%) decrease at 37 °C (*16*). In this study we therefore performed all three assays—nucleotide occlusion, Vi-induced trapping, and ATP hydrolysis—at 34 °C. The assay was carried out under basal conditions or in the presence of verapamil, 30 μM. The reaction was initiated with 5 mM ATP and quenched with 2.5% SDS; the amount of P_i released was quantified by a colorimetric method (*30*).

[α-^{32}P]ATP or ATP-γ-^{35}S Hydrolysis. ATP hydrolysis was measured by determining the amount of [α-^{32}P]ATP/ATP-γ-^{35}S hydrolyzed on the basis of a previously described assay (*32*). Purified Pgp reconstituted into liposomes (25−50 μg of protein/mL) was incubated with 200 μM [α-^{32}P]ATP or ATP-γ-^{35}S for 20 min in the ATPase buffer (see above). Liposomes without incorporated Pgp were used as controls. The reaction was stopped by adding 100 μL of ice-cold buffer containing 2.5% SDS, and 1−2 μL of this sample was spotted onto a cellulose/PEI TLC plate. TLC was carried out with 1 M HCOOH and 0.5 M LiCl as a solvent. [α-^{32}P]-ATP and [α-^{32}P]ADP were identified by exposing the dried TLC to an X-ray film and quantified by use of the STORM 860 PhosphorImager system (Molecular Dynamics, Sunnyvale, CA) and the software ImageQuaNT. In the case of ATP-γ-^{35}S, only the ATP-γ-^{35}S spot could be identified but not the ADP, as the ^{35}S was released. The amount of radionucleotide was quantified by use of a standard curve, generated by spotting known concentrations of [α-^{32}P]ATP or ATP-γ-^{35}S.

Photoaffinity Labeling with [^{125}I]IAAP. The crude membranes of High Five insect cells (100 μg) or purified and reconstituted protein (5−10 μg) were incubated at room temperature in the ATPase buffer with [^{125}I]IAAP (7 nM) for 5 min under subdued light. The samples were photo-cross-linked for 10 min at room temperature, followed by electrophoresis on 7% NuPAGE gels and quantification as described previously (*16*). Modifications to this procedure in specific experiments are detailed in the figure captions.

Photoaffinity Labeling with GPV51. The crude High Five membranes of insect cells (0.1−1 mg/mL protein) were incubated in the absence or presence of 2 mM ATP-γ-S at 34 °C for 5 min, transferred to ice, and washed by centrifugation. The resuspended pellets were treated with [^{3}H]-GPV51 in the presence of increasing concentrations of nonradioactive GPV51 for determination of apparent K_d values. Samples were irradiated on ice six times (each irradiation lasted 30 s) with a Lot-Oriel 500W mercury lamp as described previously (*33*). Vesicles were pelleted at 30000*g* for 20 min in a Beckman TL-100 ultracentrifuge at 4 °C in a TLA-100 rotor and washed in 1 mL of TS buffer. Subsequently, samples were taken up in loading buffer containing 8 M urea and 1% SDS and subjected to PAGE on 7.5% gels. After fixation and staining with Coomassie blue, bands corresponding to Pgp were excised and dissolved in 200 μL of 35% hydrogen peroxide at 95 °C for 2 h under agitation. Samples were cooled to room temperature and counted in a Packard Tricarb 2000 liquid scintillation counter. The amount of ligand associated with the Pgp band at each concentration of GPV51 is expressed in disintegrations per minute (dpm) and a measure of equilibrium binding. These values are plotted as a function of ligand concentration. It is important to note that, under the experimental conditions used, the total ligand concentration exceeds that of bound ligand by more than 3 orders of magnitude, and thus concentrations of total and free ligand can be assumed to be identical. Hyperbolic binding competitions curves were fitted to the data points by least-squares via the solver add-in of Excel software.

Occlusion of ATP-γ-S into Pgp. Crude membranes of High Five insect cells (100 μg) or purified and reconstituted protein (5−10 μg) were incubated in the ATP assay buffer (see above) with ATP-γ-S (concentrations as indicated in the figure captions) at 34 °C for 5 min. The reaction was stopped by the addition of 1 mL of ice-cold ATPase buffer, and the samples were placed on ice. Excess nucleotides were removed by centrifugation at 100000*g* for 20 min at 4 °C. The pellet was resuspended in 50 μL of ATPase buffer and used to determine 8-azido-[α-^{32}P]ATP or [^{125}I]IAAP binding as described above.

Occlusion of ATP-γ-^{35}S into Pgp. Purified and reconstituted Pgp (70 μg) was incubated in the ATP assay buffer (see above) with ATP-γ-^{35}S (concentrations as indicated in the figure captions) at 34 °C for 5 min. The reaction was stopped by the addition of 1 mL of ice-cold ATPase buffer containing 10 mM ATP, and the samples were placed on ice. Excess nucleotides were removed by centrifugation at 100000*g* for 20 min at 4 °C. The pellet was resuspended in 100 μL of ATPase buffer, and 75 μL was used to estimate the amount of protein. The protein in each sample was estimated by the method of Schaffner and Weissmann (*34*), which was specifically developed to accurately measure the concentration of membrane proteins in the presence of lipid or detergent. The amount of [^{35}S]nucleotide was also estimated in each sample. Aliquots (5 μL, in triplicate) were added to 10 mL of Bio-Safe II counting cocktail and the radioactivity was determined in a Beckman LS3801 scintillation counter. Serial dilutions of the stock ATP-γ-^{35}S solution were used to generate a standard curve, which was used to estimate the picomoles of ATP-γ-^{35}S occluded. Similarly, the protein estimated in each sample was converted to picomoles of Pgp by use of the factor 1 mg of protein = 7.14 pmol (based on a molecular mass of 140 000 Da). Together, these values were used to express the occlusion of ATP-γ-^{35}S as picomoles of ATP-γ-^{35}S per picomole of Pgp.

[α-^{32}P]ATP or [α-^{32}P]ADP Occlusion. Purified wild-type and E556Q/E1201Q mutant Pgps reconstituted into liposomes were incubated with 200 μM [α-^{32}P]ATP or [α-^{32}P]-ADP for 20 min in ATPase buffer (see above). The reaction was stopped by adding 100 μL of ice-cold buffer containing 1 M NaCl and 10 mM ATP. The sample was loaded onto a G-50 column (4 mL, diameter 1 cm) previously washed with 50 mM Tris-HCl, pH 7.5, and 0.2 M NaCl (buffer A). The proteoliposomes were eluted with buffer A and 0.25-mL fractions were collected; the fractions containing the protein were pooled, diluted to 4 mL with cold buffer A, and centrifuged at 150000*g* for 20 min. The pellet was resuspended in 15 μL of 50 mM Tris-HCl, pH 7.5, containing 2.5% SDS. Part of the sample (10 μL) was used to estimate protein by the method of Schaffner and Weissmann (*34*). In addition, 2 μL of this sample was used for TLC, and [α-^{32}P]-ATP and [α-^{32}P]ADP were identified and quantified as described above.

RESULTS

ATP and Nonhydrolyzable Analogue ATP-γ-S Have Comparable Relative Affinities for Pgp while the Nonhydrolyzable Analog AMPPNP Has an Apparently Very Low Affinity. Recent studies with several ABC proteins, both eukaryotic and prokaryotic, have suggested that an ATP-driven dimerization of the two NBDs may be a critical event in the catalytic cycle of ATP hydrolysis (*10*, *15*, *16*, *22*). The ATPase reaction in mutants of the highly conserved glutamate within the Walker B region is significantly impaired, and these mutants occlude the nucleoside triphosphate (*22*). Such mutants have been extremely useful in characterizing the ATP-driven dimer because biochemical and structural evidence suggests that the products of ATP hydrolysis, ADP and P_i, destabilize the dimer (*9*). Thus, in principle it should be possible to form the ATP-driven dimer by use of a nonhydrolyzable analogue of ATP in the wild-type protein. The results of such experiments have been mixed (see ref *10* for discussion). In order to select an appropriate nonhydrolyzable analogue of ATP, we compared the relative affinities of ATP and two commonly used nonhydrolyzable analogues, ATP-γ-S and AMPPNP for Pgp. The IC_{50} of AMPPCP for Pgp could not be determined, as even high concentrations of AMPPCP (10 mM) do not affect ATP hydrolysis or cross-linking of 8-azido-[α-^{32}P]ATP to Pgp (data not shown). Table 1 shows that ATP, AMPPNP, and ATP-γ-S all inhibit the Vi-induced trapping of 8-azido-[α-^{32}P]ADP into wild-type Pgp with IC_{50} values of 0.19, 2.8,- and 0.29 mM, respectively. In addition to using a photoaffinity probe to compare the relative affinities of the nucleotides for Pgp, we also estimated these under equilibrium conditions. Table 1 shows that the K_m(ATP) for Pgp-mediated ATP hydrolysis is 0.3 mM and the IC_{50} values for inhibition of ATP hydrolysis by AMPPNP and ATP-γ-S are 1.4 and 0.19 mM, respectively. These data indicate that the affinity of AMPPNP for Pgp is approximately 10-fold lower than that of ATP. Our data indicate that IC_{50}(AMPPNP) for inhibition of ATP hydrolysis is 1.4 mM, while IC_{50}(AMPPNP) for the inhibition of Vi-induced 8-azido-[α-^{32}P]ADP trapping is 2.8 mM. On the other hand, ATP-γ-S has an affinity for Pgp that is comparable to that of the physiological substrate, ATP.

Table 1: IC_{50} Values for Inhibition of Pgp-Mediated ATP Hydrolysis and Vi-Induced Trapping of 8-Azido-[α-^{32}P]ATP by Nonhydrolyzable ATP Analogues

	K_m(ATP hydrolysis),[a] mM	IC_{50}(ATP hydrolysis),[b] mM	IC_{50}(trapping of 8-azido-[α-^{32}P]ADP),[c] mM
ATP	0.29 ± 0.03	*d*	0.19 ± 0.02
ADP	*e*	0.61 ± 0.04	*d*
AMPPNP	*e*	1.4 ± 0.04	2.8 ± 0.09
8-azido-AMPPNP	*e*	0.16 ± 0.03	*d*
ATP-γ-S	*e*	0.19 ± 0.02	0.29 ± 0.04

[a] Pgp-mediated ATP hydrolysis was determined in the presence of increasing concentrations of ATP ranging from 0.1 to 10 mM by the colorimetric P_i release assay described under Experimental Procedures. K_m was estimated by fitting the data to the Michaelis−Menten equation by use of the software GraphPad Prism. [b] Pgp-mediated ATP hydrolysis was measured in the presence of 1 mM ATP and increasing concentrations of the ATP analogues. The Michaelis−Menten equation was used to estimate IC_{50} for inhibition of ATP hydrolysis. [c] Vi-induced trapping of 8-azido-[α-^{32}P]ADP into Pgp was determined as described under Experimental Procedures, in the presence of increasing concentrations of ATP, AMPPNP, or ATP-γ-S. The radioactivity incorporated in the Pgp band was estimated as arbitrary units by use of the STORM 860 PhosphorImager system and the software ImageQuaNT. Apparent IC_{50} values for the inhibition of Vi-induced trapping of 8-azido-[α-^{32}P]ADP were estimated by use of the curve-fitting software GraphPad Prism. Mean values (±SD) of three independent experiments are shown here. [d] Not done. [e] Not measurable.

Table 2: Comparison of Hydrolysis of ATP-γ-^{35}S and [α-^{32}P]ATP by Purified and Reconstituted Pgp

	−Pgp[a]	+Pgp[a]	−SVP[b]	+SVP[b]
[α-^{32}P]ATP hydrolysis, nmol min^{-1} (mg of Pgp)$^{-1}$	*c*	800 ± 120	*d*	*d*
ATP-γ-^{35}S hydrolysis, nmol min^{-1} (mg of Pgp)$^{-1}$	*c*	*c*	*c*	97 ± 16

[a] Pgp-mediated ATP hydrolysis was determined as conversion of [α-^{32}P]ATP to [α-^{32}P]ADP. [α-^{32}P]ATP or ATP-γ-^{35}S was incubated with purified Pgp incorporated into proteoliposomes (+Pgp) or equal volume of liposomes with no Pgp (−Pgp) in the presence of 0.03 mM verapamil for 20 min at 34 °C. The reaction was stopped by the addition of 2.5% SDS, and 2 μL samples were spotted onto a cellulose/PEI TLC plate. TLC was carried out with 1 M HCOOH and 0.5 M LiCl as solvent. In the case of [α-^{32}P]ATP, [α-^{32}P]ATP and [α-^{32}P]ADP were identified by exposing the dried TLC to an X-ray film; in the case of ATP-γ-^{35}S, only ATP-γ-^{35}S could be identified on the X-ray film. The ATP bands were quantified by use of the STORM 860 PhosphorImager system (Molecular Dynamics, Sunnyvale, CA) and the software ImageQuaNT. These values, obtained as arbitrary units, were converted to nanomoles of ATP via a standard curve. Specific activity is expressed as nanomoles of [α-^{32}P]-ATP or ATP-γ-^{35}S hydrolyzed per milligram of Pgp per minute. Mean values (±SD) of three independent experiments are depicted. [b] Snake venom phosphodiesterase- (SVP-) mediated hydrolysis of ATP-γ-^{35}S was measured by incubating ATP-γ-^{35}S (0.2 mM) in the absence (−SVP) or presence (+SVP) of 0.52 unit of SVP for 20 min at 37 °C, and the reaction was stopped by the addition of 2.5% SDS. The reaction was carried out in 50 mM Tris-HCl, pH 8, and 1 mM $MgCl_2$. The amount of ATP-γ-^{35}S hydrolyzed was quantified as described above, and specific activity is expressed as nanomoles of ATP-γ-^{35}S hydrolyzed per unit of SVP per minute. Mean values (±SD) of three independent experiments are depicted. [c] Not detected. [d] Not done.

ATP-γ-S thus appears to be a more suitable nonhydrolyzable analogue to use for studies with Pgp. However, there have been reports that ATP-γ-S may be hydrolyzed by ATPases, albeit the rate of hydrolysis is only $^1/_{200}$ that of ATP in the case of Ca^{2+} ATPase of sarcoplasmic reticulum (*35*). However, when we compared the hydrolysis of [α-^{32}P]ATP and ATP-γ-^{35}S by Pgp, we found that there was no detectable hydrolysis of ATP-γ-^{35}S after 20 min at 37 °C (Table 2). In the same time period, there was measurable hydrolysis of ATP-γ-^{35}S by purified snake venom phosphodiesterase (SVP), consistent with earlier reports of slow rates of hydrolysis of ATP-γ-S by SVP (*36*). These results suggest that ATP-γ-S can be used as a nonhydrolyzable ATP analogue when studying the transport pathway of Pgp.

Kinetics of Occlusion of ATP-γ-S into Pgp. We incubated Pgp with increasing concentrations of ATP-γ-S at either 4 or 34 °C and stopped the reaction by diluting the samples 20-fold with ice-cold buffer containing 10 mM ATP and centrifuged at 100000*g* for 20 min. This procedure ensured that the free and loosely bound ATP-γ-S would be washed off and the occluded nucleotide would remain associated with Pgp in the pellet. If ATP-γ-S was occluded in the ATP site(s), this would prevent subsequent photolabeling by 8-azido-[α-^{32}P]ATP. In Figure 1A we show that when ATP-γ-S was incubated with Pgp at 4 °C, there is minimal occlusion and the Pgp is efficiently photolabeled after the ATP-γ-S is washed off. However, when ATP-γ-S was incubated with Pgp at 34 °C, there is a concentration-dependent decrease in the level of 8-azido-[α-^{32}P]ATP photolabeling (Figure 1B), suggesting that ATP-γ-S is occluded in the ATP sites of Pgp. There is considerable evidence that Vi mimics the pentacovalent phosphorus and traps the protein in the long-lived, noncovalent ternary complex Pgp·MgADP·Vi (*37*, *38*). Thus, when we incubated Pgp in the presence of Vi and increasing concentrations of ATP prior to centrifugation, we observed inhibition of 8-azido-[α-^{32}P]ATP photolabeling (Figure 1C), similar to the finding with ATP-γ-S alone. Moreover, the IC_{50} values for inhibition of photolabeling by ATP-γ-S (alone) and ATP (in the presence of Vi) are 0.27 and 0.29 mM, respectively, comparable to the values obtained for the apparent affinities of these nucleotides for Pgp (Table 1).

Occluded ATP-γ-S and Vi-Induced Trapping of ADP Result in Reduced Affinity for Pgp-Transport Substrates. We have shown previously (*26*, *39*) that the Vi-trapped conformation of wild-type Pgp binds the photoaffinity transport-substrate analogue [^{125}I]IAAP with >30-fold reduced affinity. In addition, we have demonstrated that the double mutant of human Pgp, E556Q/E1201Q, occludes ATP in the absence of Vi and this conformation of Pgp also shows reduced binding of [^{125}I]IAAP (*16*, *19*). The reduced binding of [^{125}I]-IAAP has been interpreted as monitoring a conformational change in the transport-substrate binding from the high-affinity, ON site to a low-affinity OFF site (*25*). The temperature-dependent occlusion of ATP-γ-S shown in Figure 1 is analogous to the Vi-independent occlusion of ATP in the Walker B glutamate (E556Q/E1201Q) mutant of Pgp, a pre-hydrolysis reaction intermediate. We therefore determined the binding of [^{125}I]IAAP to Pgp after incubation with increasing concentrations of ATP-γ-S at 34 °C. Occlusion of ATP-γ-S results in reduced incorporation of [^{125}I]-IAAP with an IC_{50} of 0.25 mM. ATP, in the presence of Vi, also inhibits incorporation of [^{125}I]IAAP with a comparable IC_{50} (0.45 mM) (Figure 2A,B).

Reduced binding of photoaffinity substrates such as [^{125}I]-IAAP to demonstrate the high-affinity to low-affinity switch has been criticized on the grounds that the reaction of proteins with photoligands reflects reactivity rather than affinity (refs *40* and *41*, and see detailed discussion to address these concerns in ref *23*). The underlying reason for this phenomenon is a propensity of photoligands to preferentially react with certain amino acid residues in the protein. Thus, a decrease in cross-linking of the photoligand could reflect either a change in the affinity or a conformational change that alters the accessibility of the preferred side chain. Propafenones, in contrast to other photoligands, show minimal reaction preference, and competition of radioactively labeled photoligands by the unlabeled compound yields binding competition curves that allow determination of the concentration required for 50% occupancy of the drug-substrate site. In the absence of nucleotide, an apparent K_d of 42 μM was determined for the propafenone [^{3}H]GPV51. This K_d increased to 128 μM when the occluded nucleotide conformation of Pgp was generated with ATP-γ-S (Figure 2C). This increase was not due to changes in reactivity of the photoligands, because individual full-range displacement curves were determined for both conditions. As expected, the B_{max} values (maximal binding of GPV51) in the presence of ATP-γ-S decreased by more than 2-fold (data not given), as the concentration used for determination of B_{max} values (radiolabeled compound only) are far below the apparent K_d values.

Kinetics and Energetics of ATP-γ-^{35}S Occlusion into Human Pgp. To provide additional evidence for the coupling of ATP-γ-S occlusion at the nucleotide binding site(s) of

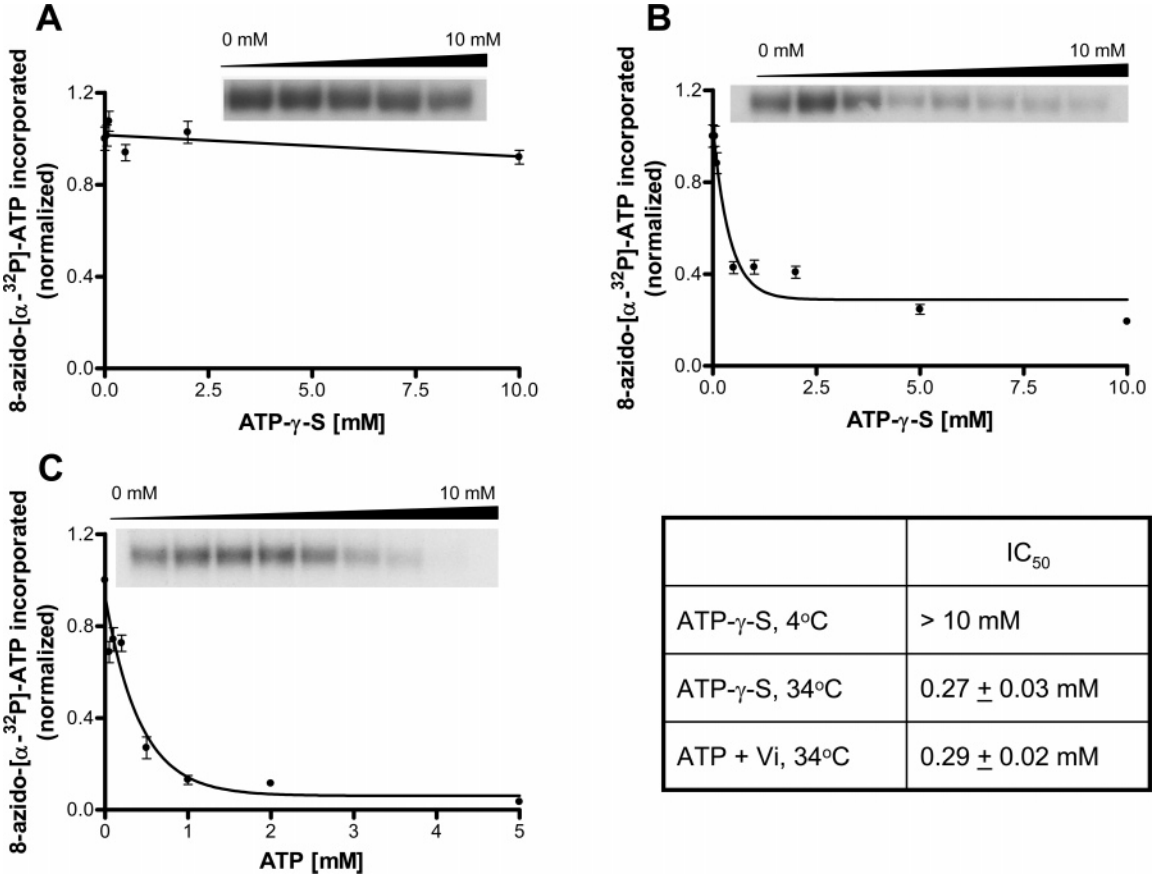

	IC_{50}
ATP-γ-S, 4°C	> 10 mM
ATP-γ-S, 34°C	0.27 ± 0.03 mM
ATP + Vi, 34°C	0.29 ± 0.02 mM

FIGURE 1: Temperature-dependent occlusion of ATP-γ-S into Pgp. Crude membranes (0.5−1.0 mg/mL) prepared from High-Five insect cells overexpressing Pgp were incubated with increasing concentrations of (A) ATP-γ-S at 4 °C, (B) ATP-γ-S at 34 °C, or (C) ATP and Vi at 34 °C for 5 min. The membranes were washed by centrifugation at 4 °C to remove excess nucleotide, resuspended in ice-cold ATPase buffer, and photo-cross-linked with 8-azido-[α-^{32}P]ATP as described under Experimental Procedures. Following electrophoresis, the radioactivity incorporated in the Pgp band was estimated as arbitraty units by use of the STORM 860 PhosphorImager system and the software ImageQuaNT. Apparent IC_{50} values for the reduced photo-cross-linked 8-azido-[α-^{32}P]ATP to Pgp preincubated with ATP-γ-S or ATP + Vi at 34 °C were estimated by use of the curve-fitting software GraphPad Prism and are shown in the table. Mean values ± SD of three independent experiments are shown in each panel. (Insets) Representative autoradiograms.

Pgp and the effect on the transport-substrate site, we used ^{35}S-labeled ATP-γ-S to characterize the temperature-dependent occlusion of a nonhydrolyzable ATP analogue. Purified Pgp reconstituted into proteoliposomes was incubated with ATP-γ-^{35}S under different conditions depicted in Figure 3A: (I) incubation at 4 °C for 5 min followed by addition of 10-fold excess ATP; (II) incubation at 34 °C for 5 min in the presence of 0.5 mM ATP-γ-^{35}S and 5 mM ATP, where ATP-γ-^{35}S and ATP were added simultaneously prior to the samples being transferred to 34 °C; (III) incubation at 34 °C for 5 min in the presence of 0.5 mM ATP-γ-^{35}S, transfer of the samples to ice and then addition of 5 mM ATP; (IV) incubation at 34 °C for 5 min in the presence of 0.5 mM ATP-γ-^{35}S + 250 μM Vi, transfer of the samples to ice, and then addition of 5 mM ATP. All samples were than diluted to 1 mL with ice-cold ATPase buffer and centrifuged at 100000*g* for 30 min. The pellets were resuspended in 2.5% SDS, and the amount of ^{35}S incorporated in each sample was determined by use of a scintillation counter. The protein in each sample was also determined by the method of Schaffner and Weissmann (*34*), which gives very accurate determinations of membrane proteins. These values could be transformed into a molar ratio of picomoles of ATP-γ-^{35}S incorporated per picomole of Pgp. This experiment shows that, at 4 °C, ATP-γ-^{35}S is fully exchangeable with ATP (Figure 3A, bar I). However, if Pgp is incubated with ATP-γ-^{35}S at 34 °C, the nonhydrolyzable nucleotide is occluded and not exchangeable with excess ATP (Figure 3A, bar III). It is important to note that if ATP-γ-^{35}S and excess ATP are simultaneously incubated with Pgp at 34 °C (Figure 3A, bar II), there is negligible incorporation of ATP-γ-^{35}S, suggesting that the nucleotide binding site is blocked by ATP and inaccessible to ATP-γ-^{35}S. Finally, Vi does not affect the occlusion of ATP-γ-^{35}S (Figure 3A, bar IV). It is also important to note that the extent of incorporation of ATP-γ-^{35}S is approximately 1 mol/mol of Pgp. We also monitored the occlusion of ATP-γ-^{35}S in the mutant and wild-type Pgps as a function of ATP-γ-^{35}S concentration (Figure 3B) and determined the molar ratio of protein: occluded nucleotide at each concentration of ATP-γ-^{35}S. This experiment provides two important pieces of information: (i) ATP-γ-^{35}S is occluded with an apparent K_d(ATP-γ-S) of 0.43 mM. This value is comparable to the affinity of ATP-γ-S for Pgp obtained by more indirect methods (Figures 1B and 2A and Table 1). Similarly, K_m(ATP) for Pgp has been reported in the literature to be within the range 0.5−1.5 mM. (ii) Also noteworthy is the fact that when the data are fit to a Langmuir isotherm, the y_{max} is 1.2. The *y*-axis in this plot represents the ratio of picomoles of nucleotide occluded per picomole of Pgp. This result suggests that the maximal

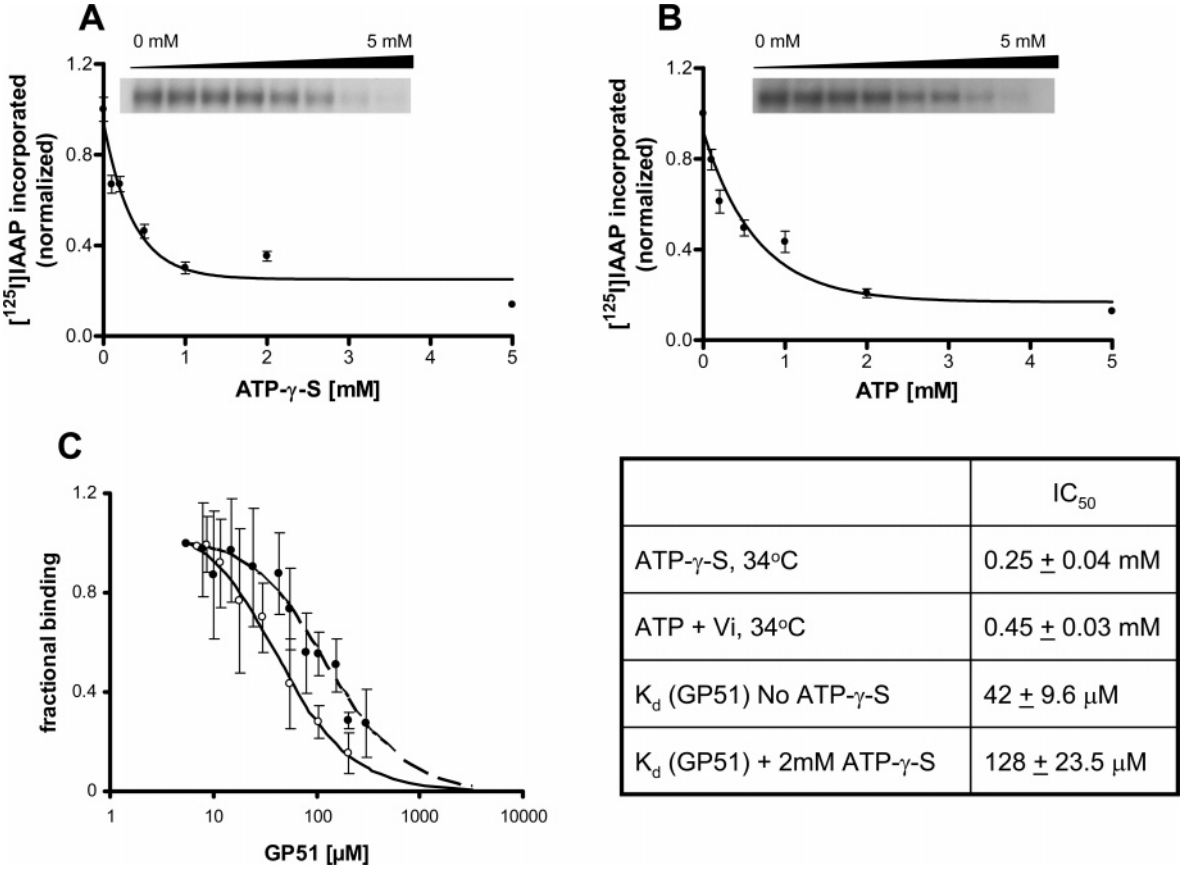

	IC_{50}
ATP-γ-S, 34°C	0.25 ± 0.04 mM
ATP + Vi, 34°C	0.45 ± 0.03 mM
K_d (GP51) No ATP-γ-S	42 ± 9.6 μM
K_d (GP51) + 2mM ATP-γ-S	128 ± 23.5 μM

FIGURE 2: Decreased affinity of transport substrate for Pgp in the occluded nucleotide conformation and in the Vi-trapped state. Crude membranes (0.5 mg/mL) prepared from High-Five insect cells overexpressing Pgp were incubated with increasing concentrations of (A) ATP-γ-S or (B) ATP and Vi at 34 °C for 5 min. The membranes were washed by centrifugation at 4 °C to remove excess nucleotide, resuspended in ice-cold ATPase buffer, and photo-cross-linked with [^{125}I]IAAP, as described under Experimental Procedures. IC_{50} for inhibition of [^{125}I]IAAP photo-cross-linking to Pgp was estimated by use of the curve-fitting software GraphPad Prism and is shown on the figure. Data points represent the mean (±SD) of three independent experiments. (C) Crude membrane from Pgp-overexpressing cells were incubated in the absence (○) and presence (●) of 2 mM ATP-γ-S for 5 min at 34 °C. The membranes were then photo-cross-linked with [^{3}H]GPV51 in the presence of increasing concentrations of non-radioactively-labeled GPV51 to determine the apparent K_d values as described under Experimental Procedures. IC_{50} values for the inhibition of [^{125}I]IAAP binding by ATP-γ-S or ATP + Vi and K_d(GPV51) in the absence of nucleotide and following incubation with ATP-γ-S at 34 °C are depicted in the table. Mean values ± SD of 3−5 independent experiments are shown. (Insets) Representative autoradiograms of incorporation of [^{125}I]IAAP into Pgp following incubation at 34 °C with indicated concentrations of ATP-γ-S or ATP (in the presence of Vi).

stoichiometry (nucleotide:protein) is approximately 1 and is consistent with earlier results obtained with Pgp mutants of the conserved glutamate in the Walker B region (*16*, *20*). These mutants show very minimal ATPase activity and occlude the nucleoside triphosphate with a protein: nucleotide ratio of 1.

The data depicted above show that occlusion of ATP-γ-S in a nonexchangeable form is temperature-dependent (compare bars I and III, Figure 3A), which also brings about an energy-dependent conformational change at the transport substrate site (Figure 2). To study the energetics of this process, we measured the occlusion of ATP-γ-^{35}S as a function of temperature (Figure 3C). Previous work has shown that, unlike ATP binding, Vi-induced trapping of nucleoside diphosphate and Vi-independent occlusion of nucleoside triphosphate in the Pgp mutant E556Q/E1201Q are both strongly temperature-dependent (*16*, *29*). Moreover, the two phenomena have comparable energetics. Recent structural and biochemical evidence has suggested that the nucleotide in the ATP binding site of an ABC transporter is flanked by the Walker A and B and the H- and Q-loops of one NBD on one side and the cavity is closed by the signature sequence and D-loop of the other NBD. Moreover, it has been suggested that the formation of such an ATP sandwich involves conformational changes that have important roles to play in the transport cycle (*16*). Using a nonhydrolyzable analogue of ATP (e.g., ATP-γ-S) with wild-type Pgp is one strategy to obtain a reaction intermediate that represents the nucleotide-driven dimerization of the two faces of the ATP-binding site.

Vi-Independent Nucleotide Occlusion Occurs in the Presence of Nucleoside Triphosphate but Not in the Presence of Nucleoside Diphosphate. Our previous work with the E556Q/E1201Q mutant human Pgp (*16*) and the data presented in this study support the view that if ATP hydrolysis cannot occur, the transporter can be locked in the ATP-bound conformation. To test this hypothesis, we compared the occlusion of 8-azido-[α-^{32}P]ATP and 8-azido-[α-^{32}P]ADP in wild-type and mutant (E556Q/E1201Q) Pgps. The wild-type Pgp shows no occlusion of nucleotide when the protein is incubated with either 8-azido-[α-^{32}P]ATP or 8-azido-[α-^{32}P]-ADP in the absence of the "transition-state analogues" Vi or BeF_x (Figure 4A, lanes 1 and 4). However, in the presence of either Vi or BeF_x incubation with either 8-azido-[α-^{32}P]-

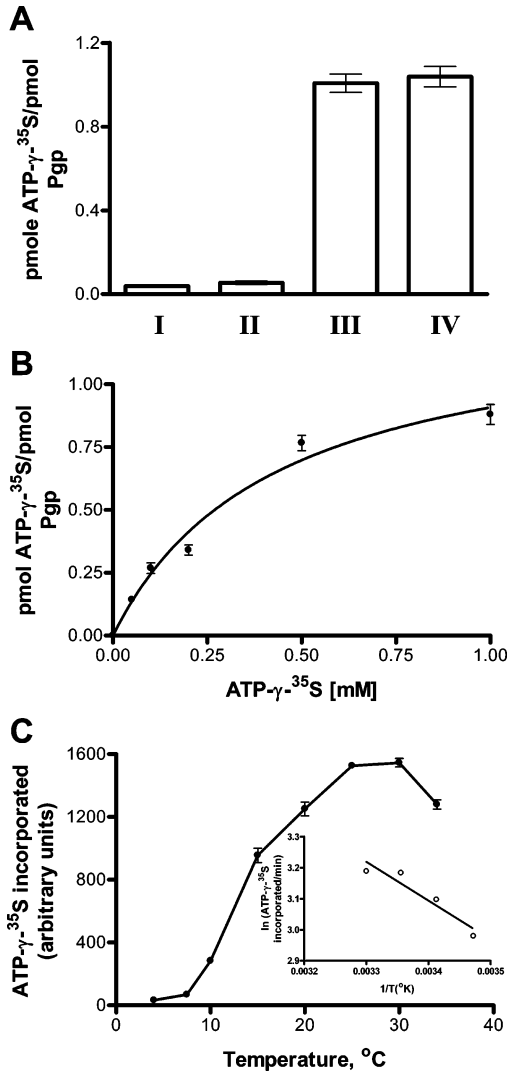

FIGURE 3: Occlusion of ATP-γ-^{35}S into Pgp. (A) Proteoliposomes reconstituted with purified Pgp (100 μg of protein/mL) were treated as follows: (I) incubated with 0.5 mM ATP-γ-^{35}S at 4 °C for 5 min, followed by addition of a 10-fold excess of ATP; (II) incubated with 0.5 mM ATP-γ-^{35}S at 34 °C for 5 min in the presence of 10-fold excess ATP and then transferred to ice; (III) incubated with 0.5 mM ATP-γ-^{35}S at 34 °C for 5 min and transferred to ice, followed by addition of 10-fold excess ATP; (IV) incubated with 0.5 mM ATP-γ-^{35}S + Vi at 34 °C for 5 min and transferred to ice, followed by addition of 10-fold excess ATP. All samples were washed by centrifugation to remove nucleotide that was not occluded or trapped and then resuspended in 2.5% SDS, and the amount of ^{35}S and protein in each sample (approximately 15−20 μg/sample) was determined by the Amido black B method (see Experimental Procedures and Results). These values could be transformed into a molar ratio of picomoles of ATP-γ-^{35}S incorporated per picomole of Pgp. (B) Purified Pgp reconstituted into proteoliposomes (approximately 25−35 μg of protein/sample) was incubated with increasing concentrations of ATP-γ-^{35}S (0.05−1 mM) at 34 °C for 5 min and transferred to ice, followed by addition of 10-fold excess ATP. The picomoles of ATP-γ-^{35}S incorporated per picomole of Pgp was estimated in each sample as described for panel A. (C) Purified Pgp reconstituted into proteoliposomes (approximately 25−35 μg of protein/sample) was incubated with 0.5 mM ATP-γ-^{35}S at varying temperatures (in the range 4−37 °C) for 5 min and transferred to ice, and 10-fold excess ATP was added. The amount of ATP-γ-^{35}S incorporated into Pgp was measured (after a wash to remove nucleotide that was not occluded) by counting samples in a liquid scintillation counter. Mean values ± SD of three independent experiments are shown. (Inset) Arrhenius plot of the data in the linear range (15−30 °C); the slope was used to calculate the activation energy (60 kJ/mol).

ATP or 8-azido-[α-^{32}P]ADP results in equivalent levels of trapping (Figure 4A, lanes 2, 3, 5, and 6). This is consistent with our previous work with Pgp (*29*) although in the case of some other transporters, such as the Tap1/Tap2 heterodimer, the trapping efficiency is considerably higher if 8-azido-[α-^{32}P]ATP and BeF_x are used rather than 8-azido-[α-^{32}P]ADP and BeF_x (*42*). The mutant Pgp (E556Q/E1201Q), on the other hand, occludes nucleotide even in the absence of Vi or BeF_x when it is incubated with 8-azido-[α-^{32}P]ATP at 34 °C (Figure 4A, lanes 7−9). Moreover, Vi and BeF_x do not affect the extent of nucleotide occlusion. These results are all consistent with previous reports (*16*, *19*, *29*, *39*). However when the mutant Pgp is incubated with 8-azido-[α-^{32}P]ADP, no occlusion of the nucleotide occurs (Figure 4A, lanes 10 and 11). Incubation of the mutant Pgp with 8-azido-[α-^{32}P]ADP in the presence of BeF_x results in some incorporation of the nucleotide (Figure 4A, lane 12) but this is less than 20% of that observed in wild-type Pgp. Our previous studies using crude membranes from HeLa cells infected with vTF7-3 and transfected with vector pTM1-*MDR1* (wild type or mutants) suggested that the double mutant (E556Q/E1201Q) occludes either 8-azido-[α-^{32}P]ATP or 8-azido-[α-^{32}P]ADP (*19*). Although infection−transfection of HeLa cells is an excellent transient expression system for transport studies, due to relatively low expression of the recombinant protein, biochemical studies are sometimes difficult to interpret. Senior and colleagues (*20*), using purified mouse Pgp expressed in *Pichia pastoris*, have also studied mutants of the conserved Walker B glutamate. These studies demonstrated that the E552Q/E1197Q mutant occludes minimal amounts of [^{14}C]ADP after an extended incubation of 120 min [see Figure 5 in (*20*)]. We therefore compared the occlusion of [α-^{32}P]ATP and [α-^{32}P]ADP into wild-type Pgp and the mutant E556Q/E1201Q using purified human Pgp reconstituted into proteoliposomes. Figure 4B shows that both [α-^{32}P]ATP and [α-^{32}P]ADP are trapped into wild-type Pgp, but only in the presence of Vi. The mutant Pgp, E556Q/E1201Q, occludes [α-^{32}P]ATP in the absence of Vi but shows minimal occlusion of [α-^{32}P]ADP. A time course of [α-^{32}P]ATP occlusion shows a $t_{1/2}$ of 1.6 min (Figure 4C). We extended the time of incubation to 60 min but observed no significant occlusion of [α-^{32}P]ADP (Figure 4C, inset). Similarly, we show that while occlusion of [α-^{32}P]-ATP is strongly temperature-dependent (Figure 4D), there is a very slight increase in the occlusion of [α-^{32}P]ADP from 15 to 37 °C. These data clearly demonstrate that there is minimal occlusion of [α-^{32}P]ADP which is not significantly dependent on temperature. Finally we show (Figure 5) that the relative affinities of nucleoside triphosphate and nucleoside diphosphate for the mutant (E556Q/E1201Q) Pgp do not provide the explanation for the lack of occlusion of ADP. We show that the concentrations of 8-azido-[α-^{32}P]ATP and 8-azido-[α-^{32}P]ADP required for half-maximal incorporation into Pgp are comparable (12 and 21 μM, respectively) (Figure 5A). Similarly, ATP and ADP both inhibit the cross-linking of 8-azido-[α-^{32}P]ATP to the mutant Pgp with IC_{50} values of 0.65 ± 0.07 and 0.29 ± 0.04 mM, respectively (Figure 5B). We next compared the occlusion of ATP and ADP into the mutant Pgp (E556Q/E1201Q). Purified reconstituted mutant Pgp was incubated for 5 min at 37 °C in the presence of increasing concentrations of either ATP or ADP. The reaction was stopped by adding ice-cold ATPase buffer and

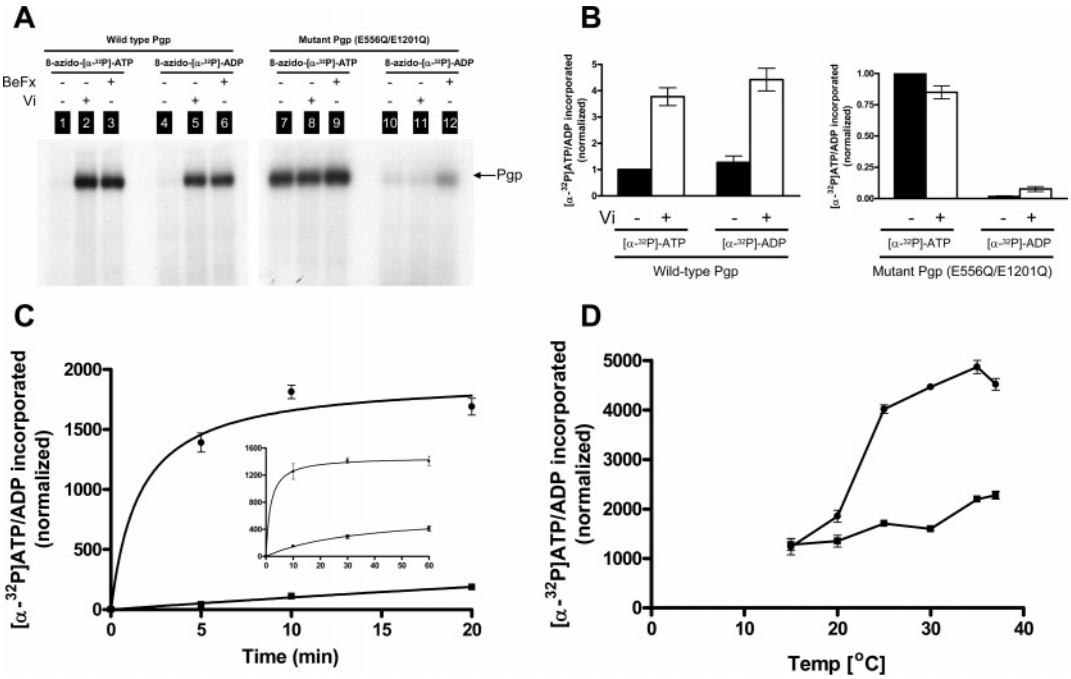

FIGURE 4: Occlusion of nucleoside triphosphates and nucleoside diphosphates in mutant (E556Q/E1201Q) Pgp. (A) Purified Pgps (wild type and E556Q/E1201Q mutant) reconstituted into proteoliposomes (100 μg/mL) were incubated with 50 μM 8-azido-[α-^{32}P]ATP or 50 μM 8-azido-[α-^{32}P]ADP either alone or in the presence of Vi or BeF_x at 34 °C for 5 min. Samples were transferred to ice, photo-cross-linked, and subjected to gel electrophoresis. The dried gel was exposed to an X-ray film, and a typical autoradiogram with the reaction conditions is depicted. (B) Purified Pgps (wild type and E556Q/E1201Q mutant) reconstituted into proteoliposomes (25−30 μg/assay) were incubated with 200 μM [α-^{32}P]ATP or [α-^{32}P]ADP either alone (solid bars) or in the presence of Vi (open bars) at 34 °C for 5 min. The reaction was stopped by adding 100 μL of ice-cold buffer containing 1 M NaCl and 10 mM ATP. Free nucleotides were removed by size-exclusion chromatography and centrifugation as described under Experimental Procedures. Radioactivity retained in each sample was estimated by use of a scintillation counter and corrected for amount of protein. The data were normalized such that for both wild-type and mutant Pgps, [α-^{32}P]ATP incorporated in the absence of Vi was taken to be 1. (C) Occlusion of [α-^{32}P]ATP or [α-^{32}P]ADP into the E556Q/E1201Q mutant Pgp was monitored as a function of time as described for panel B. Data were normalized for protein, and the radioactivity at time ($t = 0$) was subtracted from the data set. (Inset) Extended incubation up to 1 h. $t_{1/2}$ for occlusion of [α-^{32}P]ATP was determined to be 1.6 min; however, it was not possible to estimate $t_{1/2}$ for occlusion of [α-^{32}P]ADP. (D) Occlusion of [α-^{32}P]ATP (●) or [α-^{32}P]ADP (■) into the E556Q/E1201Q mutant Pgp was monitored as a function of temperature as described for panel B. Data were normalized for the amount of protein recovered in each sample at the end of the assay. All experiments were performed in triplicate and the mean values (±SD) are plotted. Note [α-^{32}P]ADP was prepared from [α-^{32}P]ATP by incubation with hexokinase and D-glucose as described previously (*15*). Conversion of [α-^{32}P]ATP to [α-^{32}P]ADP was monitored by TLC, and stock solutions of both had the same specific activity. This was confirmed by measuring the radioactivity of the stock solutions.

transferring to ice. Nucleotides that were not occluded were removed by centrifugation at 100000*g*, and the proteoliposomes were resuspended into the ATPase buffer. These samples were incubated with 10 μM 8-azido-[α-^{32}P]ATP for 5 min on ice and irradiated at 365 nm. In this assay, occluded nucleotides would not allow photo-cross-linking of 8-azido-[α-^{32}P]ATP. When the mutant Pgp is treated with ADP, the ADP binds to the ATP site but is not occluded and is therefore washed off and 8-azido-[α-^{32}P]ATP can cross-link unhindered. On the other hand, ATP is occluded, cannot be washed off, and inhibits the cross-linking of 8-azido-[α-^{32}P]-ATP in a concentration-dependent manner (Figure 5C). These data demonstrate that while ATP is occluded into the mutant Pgp (IC_{50} for inhibition of 8-azido-[α-^{32}P]ATP cross-linking, 0.32 mM), there is almost no occlusion of ADP even at a concentration of 10 mM. The results thus suggest that while the nucleoside triphosphate can bring about the dimerization of the apposing faces of the NBD, such a dimerization is not favored in the presence of the nucleoside diphosphate.

DISCUSSION

Recent studies have led to the concept of ATP-driven dimerization in ABC proteins where the nucleotide permits the association of the two halves of the ATP site. In the case of Pgp, experimental evidence suggests the existence of three distinct transition states: ATP bound, ATP occluded, and ADP-Vi trapped (for reviews see refs *22* and *23*). These distinctions are important, because it has been suggested that conformational changes that accompany the formation of the dimer are coupled to a high-affinity to low-affinity switch at the transport-substrate site (*6*). The nonhydrolyzable ATP analogues AMPPNP and ATP-γ-S have been used by several groups to argue that ATP binding rather than hydrolysis represents the step in the catalytic cycle of Pgp at which a high-affinity to low-affinity switch occurs (*6*, *43*−*47*). However, these studies do not distinguish between the ATP bound and ATP occluded states. The occluded nucleotide conformation (*16*, *22*) has been characterized by using mutants of the conserved glutamate in Walker B (E556Q/E1201Q in human Pgp) but not by using nonhydrolyzable ATP analogues. Using nonhydrolyzable ATP analogues to generate the occluded nucleotide conformation of Pgp would permit the use of wild-type protein. This is particularly important in understanding the coupling between conformational changes at the TMDs during different steps of the ATPase reaction, where the mutant Pgp could have subtle

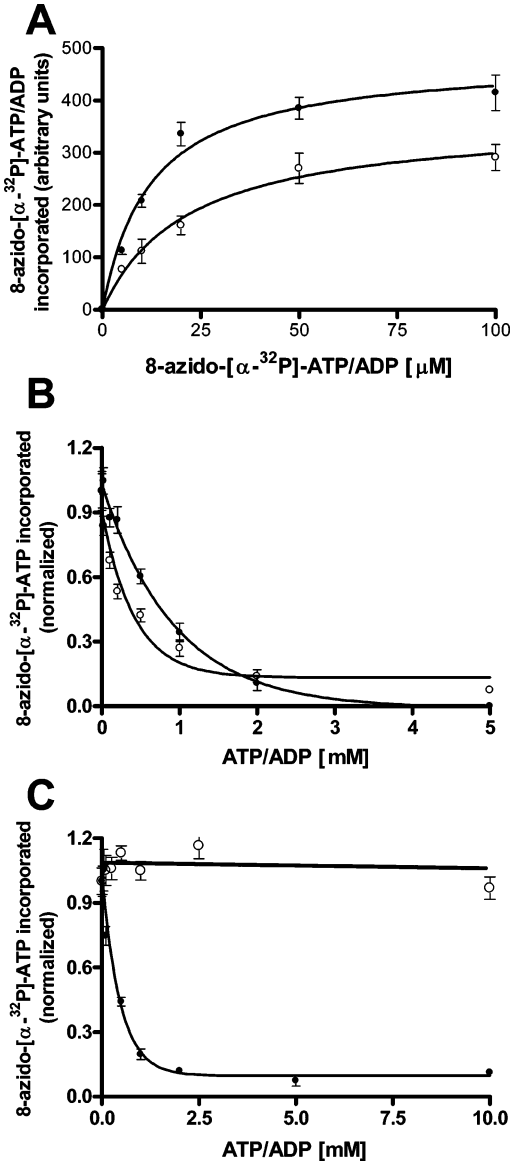

FIGURE 5: Determination of the affinities of nucleotides for the E556Q/E1201Q mutant Pgp. (A) Apparent K_d(8-azido-ATP/8-azido-ADP) for Pgp was estimated by determining the photolabeling of reconstituted purified mutant Pgp (E556Q/E1201Q) in the presence of increasing concentrations of 8-azido-[α-^{32}P]ATP (●) or 8-azido-[α-^{32}P]ADP (○) at 4 °C, as described under Experimental Procedures. (B) Apparent affinities of ATP and ADP were estimated by incubating increasing concentrations of either ATP (●) or ADP (○) with purified reconstituted mutant (E556Q/E1201Q) Pgp (5−10 μg of protein) and 10 μM 8-azido-[α-^{32}P]ATP (8−10 μCi/nmol) at 4 °C, followed by irradiation at 365 nm on ice for 5 min. Following electrophoresis, the radioactivity incorporated in the Pgp bands was estimated as described under Experimental Procedures. (C) Purified reconstituted mutant (E556Q/E1201Q) Pgp (25−35 μg of protein) was incubated with increasing concentrations of either ATP (●) or ADP (○) at 34 °C for 5 min. The reaction was stopped by the addition of ice-cold buffer, and excess unoccluded nucleotides were removed by centrifugation at 100000*g*. The pellet was resuspended in ATPase buffer, incubated with 10 μM 8-azido-[α-^{32}P]ATP (8−10 μCi/nmol) at 4 °C, and irradiated at 365 nm for 5 min on ice. Following electrophoresis, the radioactivity incorporated in the Pgp bands was estimated as described under Experimental Procedures. Curve-fitting was performed with the software GraphPad Prism. Mean values ± SD of three independent experiments are depicted.

effects on folding. The difficulty in obtaining occlusion of nonhydrolyzable ATP analogues has been attributed to "subtle electrostatic and steric differences" between nucleotides (*9*). Thus, the choice of a particular nonhydrolyzable ATP analogue and a careful characterization of the conformer generated are both necessary. We found that while ATP and ATP-γ-S inhibit Vi-induced trapping of 8-azido-[α-^{32}P]ATP into Pgp with comparable IC_{50} values, almost 10-fold higher concentrations of AMP-PNP are required (Table 1) and AMPPCP is not recognized by human Pgp (data not shown). However, AMP-PNP is often preferred over ATP-γ-S, as there have been reports that some ATPases do hydrolyze ATP-γ-S, albeit at a very slow rate (*36*). The difference between the affinities of AMP-PNP and ATP-γ-S is almost an order of magnitude, so ATP-γ-S would be the preferred analogue to use. We therefore determined that under the conditions used in this study there was no detectable hydrolysis of ATP-γ-S by Pgp (Table 2). It is of course possible that ATP-γ-S is hydrolyzed at a rate that is too slow to be detected; it would, however, be "nonhydrolyzable" for the purpose of our assays. We also demonstrate that ATP-γ-S interacts with Pgp at the nucleotide binding site(s) to displace ATP and 8-azido-[α-^{32}P]ATP (Table 1) in a concentration-dependent manner. Previous work with the E556Q/E1201Q mutant of Pgp showed that occlusion of the nucleoside triphosphate has an activation energy of approximately 50 kJ/mol (*16*). Similarly, the E599Q mutant of the mitochondrial transporter Mdl1 exhibits ATP-driven dimerization with an activation energy of approximately 70 kJ/mol (*17*). Thus, if ATP-γ-S drives a similar stable association of the ATP-binding pocket, it should be energy-(temperature-) dependent and result in occlusion of the ATP-γ-S. We found that although ATP-γ-S binds to the ATP site at 4 °C, there is no stable occlusion (Figure 1A), as the bound ATP-γ-S is competed by excess ATP. However, at 34 °C, a stable, concentration-dependent occlusion (Figure 1B) of ATP-γ-S is observed, which is comparable to the trapping of ADP in the presence of Vi (Figure 1C). The fact that the IC_{50} values obtained for the occlusion of ATP-γ-S (Figure 1B) and ADP/Vi (Figure 1C) are comparable to the apparent affinities of these nucleotides for Pgp suggests that the assay reflects the conformational changes occurring under equilibrium conditions and not effects on the photo-cross-linking of the photoaffinity probes. Moreover, though these experiments were carried out at different temperatures, photo-cross-linking was carried out over ice in all instances. Thus these experiments allow Pgp to be trapped into stable reaction intermediates under equilibrium conditions, and conformational changes at the ATP binding site are reported by use of the photoaffinity analogue of ATP, 8-azido-[α-^{32}P]ATP.

We reported earlier that the mutant Pgp, E556Q/E1201Q, in the occluded nucleotide conformation brings about the high-affinity to low-affinity switch (*16*). The data presented above suggest that by use of ATP-γ-S it is possible to arrest wild-type Pgp at the same or an equivalent step in the catalytic cycle. We monitored the photo-cross-linking of the Pgp transport-substrate, [^{125}I]IAAP, following incubation with ATP-γ-S at 34 °C, and we show that there is a concentration-dependent decrease in cross-linking of IAAP (Figure 2A). A comparable decrease in the cross-linking of [^{125}I]IAAP occurs when Pgp is incubated with increasing concentrations of ATP in the presence of 0.25 mM Vi at 34 °C. Moreover, the IC_{50} values for the inhibition of [^{125}I]IAAP binding and occlusion of ATP-γ-S are comparable (compare Figures 1B

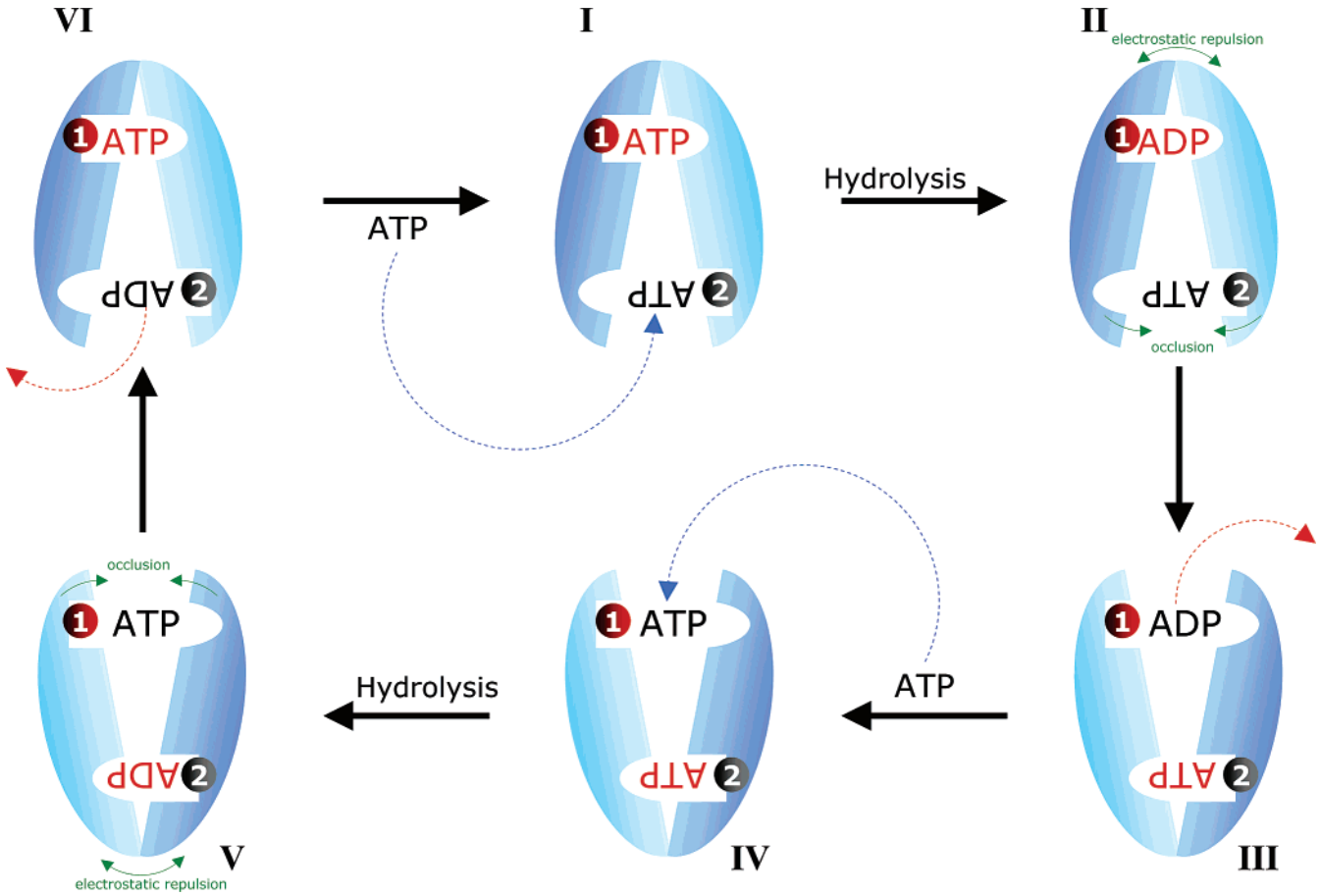

FIGURE 6: Occluded nucleotide conformation of Pgp and catalytic cycle of ATP hydrolysis. The occluded nucleotide conformation may provide a basis for the alternate catalysis hypothesis for the catalytic cycle of Pgp-mediated ATP hydrolysis. The two ATP sites are labeled 1 and 2 in red and black circles, respectively. The nucleotide that is undergoing ATP hydrolysis is shown in red. Blue dashed arrows show entry of ATP, and red dashed arrows show release of ADP. Step I represents the occluded nucleotide conformation (see Figure 1 in ref *23* for the distinction between an open dimer, a symmetric ATP bound state, and an asymmetric occluded nucleotide state). In this conformation one of the two ATPs (depicted in red) is occluded at ATP site 1. Only the ATP that was occluded in step I is hydrolyzed to ADP (step II). Formation of ADP results in disassociation of the apposing faces of the ATP pocket, resulting in the release of ADP (steps II and III) from the ATP site 1. This is consistent with the data presented in Figure 4. Dissociation of nucleotide at one ATP site is accompanied by occlusion of ATP at site 2, the alternate site (steps II and III). Concomitantly ATP is bound (ATP in black) but not occluded at the site where ADP was released (step IV). The occluded ATP at site 2 is then hydrolyzed, followed by dissociation of the ATP site and release of ADP (steps V and VI). At step I or IV, where nucleotide is occluded, there is a conformational change in the transmembrane drug-substrate binding site, resulting in reduced affinity for the transport substrate (*16*). The occluded nucleotide (E·S) can be obtained either by use of wild-type Pgp and ATP-γ-S (Figures 1−3) or by use of the Walker B, E556Q/E1201Q double mutant of human Pgp (*16*, *22*, *23*).

and 2A). In addition, we also used the propafenone GPV51, which in contrast to [^{125}I]IAAP shows minimal reaction preference, and competition of radioactively labeled photoligands by the unlabeled compound yields binding competition curves that allow determination of the concentration required for 50% occupancy of the drug-substrate site. In the absence of nucleotide, an apparent K_d of 42 μM was determined. This K_d increased to 128 μM when the occluded nucleotide conformation of Pgp was generated by use of ATP-γ-S (Figure 2C). This increase was not due to changes in reactivity of the photoligands, because individual full-range displacement curves were determined for both conditions. These studies thus show that occlusion of ATP-γ-S results in reduced affinity for the transport-substrate. An earlier report by Callaghan and co-workers (*43*) also showed that incubation of Pgp with ATP-γ-S at 37 °C had a profound effect on the binding capacity of [^{3}H]vinblastine. Similarly, experiments with permeabilized intact cells showed that treatment with ATP-γ-S showed the greatest decrease in reactivity to UIC2, a conformation-sensitive monoclonal antibody (*48*).

Recent studies show that in Pgp the "occluded" state contains only 1 mol of ATP/mol of Pgp. Similar results were obtained in studies of the effect of ATP-γ-S on UIC2 reactivity in intact cells, where the Hill number for ATP-γ-S was found to be 1.02 ± 0.13 (*48*). A molecular dynamics simulation of the ATP binding process in BtuCD (an ABC transporter that is the vitamin B_{12} importer in *E. coli*) favors the idea that, following the formation of a nucleotide sandwich, the protein undergoes conformational changes to an asymmetric occluded state (*49*). This study found that if both nucleotides were docked in identical positions relative to Walker A and B of each NBD, MgATP binding occurred across the dimer interface of one NBD. At the other NBD, the binding pocket actually opened up, preventing the formation of hydrogen bonds between ATP and the signature motif of the apposing cassette. The results were more ambiguous when the simulations were performed with MalK, the nucleotide binding domain of the maltose transporter (*14*). The authors suggest that the presence of TMDs may be required for asymmetric nucleotide binding. Previous studies

with Walker B glutamate mutants of Pgp (E556Q/E1201Q in human and E552A/E1197A in mouse) have characterized the occluded nucleotide conformation (*16*, *19*−*22*). The trapped nucleotide is predominantly the nucleoside triphosphate, the occlusion is temperature-dependent, and the maximal stoichiometry (MgATP:Pgp) is 1:1. We show in Figure 3A, using ATP-γ-^{35}S, that occlusion is strongly temperature-dependent, comparable to the occlusion of [α-^{32}P]ATP in the mutant human Pgp, E556Q/E1201Q. Moreover, the maximal stoichiometry of occlusion at 34 °C is 1 mol of ATP-γ-^{35}S/mol of Pgp (Figure 3B).

Thus, it is clear from our data that ATP-γ-S can be used to obtain the occluded nucleotide conformation with wild-type Pgp, an intermediate that is structurally and energetically distinct from the symmetrical dimer. Moreover, although the molecular basis for alternating catalysis is poorly understood, recent structural studies, real-time molecular dynamics simulations, and characterization of occluded nucleotide conformation of Pgp (described above) provide important clues. Several crystal structures of isolated NBDs show an ATP-driven dimer (*10*, *11*, *50*). Second, this stage in the reaction pathway appears to be a transition state, dimerization of NBDs being rapidly followed by the asymmetric occlusion of ATP at one of the two ATP sites (see Figure 1 in ref *23*). Finally, several studies suggest that hydrolysis of ATP (i.e., presence of ADP at the active site) leads to the dissociation of the dimer (*51*). The model depicted in Figure 6 endeavors to explain these findings in the context of a mechanism for alternating catalysis. Pgp in the asymmetric occluded nucleotide conformation is the starting point of the cycle (step I). Occlusion of ATP is followed by hydrolysis, resulting in the active site being occupied by ADP (step II). Evidence from bacterial systems suggests that a NBD occupied by ADP is unstable and dissociates due to electrostatic repulsion (*9*, *10*, *51*). Similarly, we find that the Pgp mutant (E556Q/E1201Q) occludes 8-azido-[α-^{32}P]ATP in the absence of Vi or BeF_x, although the mutant Pgp cannot occlude 8-azido-[α-^{32}P]ADP or [α-^{32}P]ADP (Figure 4). Thus the product of the ATPase reaction, ADP, would bring about dissociation of the ATP site where hydrolysis occurred (steps II and III). Moreover, if the second ATP were retained in a loosely bound state during occlusion, as suggested by Tombline and Senior and co-workers (*20*−*22*), dissociation at the first catalytic site could result in occlusion of ATP at the second (steps II and III). Following release of ADP from the first catalytic site, this site would be occupied by ATP, albeit loosely (step IV). The next ATP hydrolysis event would occur at the second or alternate catalytic site where ATP is now occluded (step V), resulting in electrostatic repulsion and opening of the site (step VI). Thus, the asymmetric occlusion of ATP at one ATP site may be instrumental in bringing about alternate catalysis. Additional support for this view comes from the recently solved structure of Sav1866, a multidrug transporter from *S. aureus* (*52*). This structure deviates from all previous structures in that the transmembrane helices are not aligned side by side but are intricately interleaved, and their maximal separation during the catalytic cycle is likely to be limited. Thus, mechanistic models that suggest complete association and dissociation of the NBDs may be unlikely in full-length proteins (*53*), which is consistent with the model presented here.

In this study, we have generated the occluded nucleotide conformation in wild-type Pgp, akin to the E·S state of the ATPase reaction, using the nonhydrolyzable ATP analogue ATP-γ-S, thus eliminating the need for Walker B mutants. Our data suggest that the asymmetrical occlusion of ATP is distinct from the nucleotide-bound state of the protein and may also be different from the symmetric closed dimer observed in crystal structures of isolated NBDs of ABC proteins. Furthermore, the formation of the occluded nucleotide conformation during the progression of the ATPase reaction may result in alternating catalysis at the two ATP sites. Finally, this step in the catalytic pathway also appears to have an important role in the transport cycle as the high-affinity to low-affinity switch at the TMDs occurs during the formation of the occluded nucleotide conformation. This is consistent with the suggestion made recently by Aanismaa and Seelig (*54*) that drug release from the TMDs occurs before ATP is hydrolyzed.

ACKNOWLEDGMENT

We thank Michael M. Gottesman for discussions and encouragement and George Leiman for editorial assistance.

REFERENCES

1. Dean, M., and Annilo, T. (2005) Evolution of the ATP-binding cassette (ABC) transporter superfamily in vertebrates. *Annu. Rev. Genomics Hum. Genet. 6*, 123−142.
2. Gottesman, M. M., and Ambudkar, S. V. (2001) Overview: ABC transporters and human disease. *J. Bioenerg. Biomembr. 33*, 453−458.
3. Gottesman, M. M., Fojo, T., and Bates, S. E. (2002) Multidrug resistance in cancer: role of ATP-dependent transporters. *Nat. Rev. Cancer 2*, 48−58.
4. Ambudkar, S. V., Kim, I. W., Xia, D., and Sauna, Z. E. (2006) The A-loop, a novel conserved aromatic acid subdomain upstream of the Walker A motif in ABC transporters, is critical for ATP binding. *FEBS Lett. 580*, 1049−1055.
5. Ambudkar, S. V., Kim, I. W., and Sauna, Z. E. (2006) The power of the pump: Mechanisms of action of P-glycoprotein (ABCB1). *Eur. J. Pharm. Sci. 27*, 392−400.
6. Higgins, C. F., and Linton, K. J. (2004) The ATP switch model for ABC transporters. *Nat. Struct. Mol. Biol. 11*, 918−926.
7. Jones, P. M., and George, A. M. (1999) Subunit interactions in ABC transporters: towards a functional architecture. *FEMS Microbiol. Lett. 179*, 187−202.
8. Hung, L. W., Wang, I. X. Y., Nikaido, K., Liu, P. Q., Ames, G. F. L., and Kim, S. H. (1998) Crystal structure of the ATP-binding subunit of an ABC transporter. *Nature 396*, 703−707.
9. Moody, J. E., Millen, L., Binns, D., Hunt, J. F., and Thomas, P. J. (2002) Cooperative, ATP-dependent Association of the Nucleotide Binding Cassettes during the Catalytic Cycle of ATP-binding Cassette Transporters. *J. Biol. Chem. 277*, 21111−21114.
10. Smith, P. C., Karpowich, N., Millen, L., Moody, J. E., Rosen, J., Thomas, P. J., and Hunt, J. F. (2002) ATP Binding to the Motor Domain from an ABC Transporter Drives Formation of a Nucleotide Sandwich Dimer. *Mol. Cell 10*, 139−149.
11. Chen, J., Lu, G., Lin, J., Davidson, A. L., and Quiocho, F. A. (2003) A tweezers-like motion of the ATP-binding cassette dimer in an ABC transport cycle. *Mol. Cell 12*, 651−661.
12. Zaitseva, J., Jenewein, S., Wiedenmann, A., Benabdelhak, H., Holland, I. B., and Schmitt, L. (2005) Functional characterization and ATP-induced dimerization of the isolated ABC-domain of the haemolysin B transporter. *Biochemistry 44*, 9680−9690.
13. Zaitseva, J., Oswald, C., Jumpertz, T., Jenewein, S., Wiedenmann, A., Holland, I. B., and Schmitt, L. (2006) A structural analysis of asymmetry required for catalytic activity of an ABC-ATPase domain dimer. *EMBO J. 25*, 3432−3443.
14. Oloo, E. O., Fung, E. Y., and Tieleman, D. P. (2006) The Dynamics of the MgATP-driven Closure of MalK, the Energy-transducing Subunit of the Maltose ABC Transporter. *J. Biol. Chem. 281*, 28397−28407.

15. Janas, E., Hofacker, M., Chen, M., Gompf, S., van der Does, C., and Tampe, R. (2003) The ATP Hydrolysis Cycle of the Nucleotide-binding Domain of the Mitochondrial ATP-binding Cassette Transporter Mdl1p. *J. Biol. Chem. 278*, 26862−26869.
16. Sauna, Z. E., Nandigama, K., and Ambudkar, S. V. (2006) Exploiting reaction intermediates of the ATPase reaction to elucidate the mechanism of transport by P-glycoprotein (ABCB1). *J. Biol. Chem. 281*, 26501−26511.
17. van der Does, C., Presenti, C., Schulze, K., Dinkelaker, S., and Tampe, R. (2006) Kinetics of the ATP hydrolysis cycle of the nucleotide-binding domain of Mdl1 studied by a novel site-specific labeling technique. *J. Biol. Chem. 281*, 5694−5701.
18. Al-Shawi, M. K., Polar, M. K., Omote, H., and Figler, R. A. (2003) Transition state analysis of the coupling of drug transport to ATP hydrolysis by P-glycoprotein. *J. Biol. Chem. 278*, 52629−52640.
19. Sauna, Z. E., Muller, M., Peng, X. H., and Ambudkar, S. V. (2002) Importance of the conserved Walker B glutamate residues, 556 and 1201, for the completion of the catalytic cycle of ATP hydrolysis by human P-glycoprotein (ABCB1). *Biochemistry 41*, 13989−14000.
20. Tombline, G., Bartholomew, L. A., Urbatsch, I. L., and Senior, A. E. (2004) Combined mutation of catalytic glutamate residues in the two nucleotide binding domains of P-glycoprotein generates a conformation that binds ATP and ADP tightly. *J. Biol. Chem. 279*, 31212−31220.
21. Tombline, G., Muharemagic, A., White, L. B., and Senior, A. E. (2005) Involvement of the "occluded nucleotide conformation" of P-glycoprotein in the catalytic pathway. *Biochemistry 44*, 12879−12886.
22. Tombline, G., and Senior, A. E. (2005) The occluded nucleotide conformation of P-glycoprotein. *J. Bioenerg. Biomembr. 37*, 497−500.
23. Sauna, Z. E., and Ambudkar, S. V. (2007) About a switch: how P-glycoprotein (ABCB1) harnesses the energy of ATP binding and hydrolysis to do mechanical work. *Mol. Cancer Ther. 6*, 13−23.
24. Senior, A. E., Al-Shawi, M. K., and Urbatsch, I. L. (1995) The catalytic cycle of P-glycoprotein. *FEBS Lett. 377*, 285−289.
25. Ramachandra, M., Ambudkar, S. V., Chen, D., Hrycyna, C. A., Dey, S., Gottesman, M. M., and Pastan, I. (1998) Human P-glycoprotein exhibits reduced affinity for substrates during a catalytic transition state. *Biochemistry 37*, 5010−5019.
26. Sauna, Z. E., and Ambudkar, S. V. (2000) Evidence for a requirement for ATP hydrolysis at two distinct steps during a single turnover of the catalytic cycle of human P-glycoprotein. *Proc. Natl. Acad. Sci. U.S.A. 97*, 2515−2520.
27. Kerr, K. M., Sauna, Z. E., and Ambudkar, S. V. (2001) Correlation between steady-state ATP hydrolysis and vanadate-induced ADP trapping in human P-glycoprotein. Evidence for ADP release as the rate-limiting step in the catalytic cycle and its modulation by substrates. *J. Biol. Chem. 276*, 8657−8664.
28. Sauna, Z. E., Smith, M. M., Muller, M., and Ambudkar, S. V. (2001) Evidence for the vectorial nature of drug (substrate)-stimulated ATP hydrolysis by human P-glycoprotein. *J. Biol. Chem. 276*, 33301−33304.
29. Sauna, Z. E., Smith, M. M., Muller, M., and Ambudkar, S. V. (2001) Functionally similar vanadate-induced 8-azidoadenosine 5′-[α-^{32}P]diphosphate-trapped transition state intermediates of human P-glycoprotein are generated in the absence and presence of ATP hydrolysis. *J. Biol. Chem. 276*, 21199−21208.
30. Ambudkar, S. V. (1998) Drug-stimulatable ATPase activity in crude membranes of human MDR1-transfected mammalian cells. *Methods Enzymol. 292*, 504−514.
31. Ambudkar, S. V., Lelong, I. H., Zhang, J., Cardarelli, C. O., Gottesman, M. M., and Pastan, I. (1992) Partial purification and reconstitution of the human multidrug-resistance pump: characterization of the drug-stimulatable ATP hydrolysis. *Proc. Natl. Acad. Sci. U.S.A. 89*, 8472−8476.
32. Kozak, L., Gopal, G., Yoon, J. H., Sauna, Z. E., Ambudkar, S. V., Thakurta, A. G., and Dhar, R. (2002) Elf1p, a member of the ABC class of ATPases, functions as a mRNA export factor in *Schizosaccharomyces pombe*. *J. Biol. Chem. 277*, 33580−33589.
33. Pleban, K., Kopp, S., Csaszar, E., Peer, M., Hrebicek, T., Rizzi, A., Ecker, G. F., and Chiba, P. (2005) P-glycoprotein substrate binding domains are located at the transmembrane domain/transmembrane domain interfaces: A combined photoaffinity labeling-protein homology modeling approach. *Mol. Pharmacol. 67*, 365−374.
34. Schaffner, W., and Weissmann, C. (1973) A rapid, sensitive, and specific method for the determination of protein in dilute solution. *Anal. Biochem. 56*, 502−514.
35. Yasuoka, K., Kawakita, M., and Kaziro, Y. (1982) Interaction of Adenosine-5′-*O*-(3-Thiotriphosphate) with Ca^{2+},Mg^{2+}-Adenosine Triphosphatase of Sarcoplasmic Reticulum. *J. Biochem. (Tokyo) 91*, 1629−1637.
36. Eckstein, F. (1985) Nucleoside Phosphorothioates. *Annu. Rev. Biochem. 54*, 367−402.
37. Urbatsch, I. L., Sankaran, B., Weber, J., and Senior, A. E. (1995) P-glycoprotein is stably inhibited by vanadate-induced trapping of nucleotide at a single catalytic site. *J. Biol. Chem. 270*, 19383−19390.
38. Sauna, Z. E., Smith, M. M., Muller, M., Kerr, K. M., and Ambudkar, S. V. (2001) The mechanism of action of multidrug-resistance-linked P-glycoprotein. *J. Bioenerg. Biomembr. 33*, 481−491.
39. Sauna, Z. E., and Ambudkar, S. V. (2001) Characterization of the catalytic cycle of ATP hydrolysis by human P-glycoprotein: The two ATP hydrolysis events in a single catalytic cycle are kinetically similar but affect different functional outcomes. *J. Biol. Chem. 276*, 11653−11661.
40. Qu, Q., Chu, J. W. K., and Sharom, F. J. (2003) Transition state P-glycoprotein binds drugs and modulators with unchanged affinity, suggesting a concerted transport mechanism. *Biochemistry 42*, 1345−1353.
41. Russell, P. L., and Sharom, F. J. (2006) Conformational and functional characterization of trapped complexes of the P-glycoprotein multidrug transporter. *Biochem. J. 399*, 315−323.
42. Chen, M., Abele, R., and Tampe, R. (2003) Peptides induce ATP hydrolysis at both subunits of the transporter associated with antigen processing. *J. Biol. Chem. 278*, 29686−29692.
43. Martin, C., Berridge, G., Mistry, P., Higgins, C., Charlton, P., and Callaghan, R. (2000) Drug binding sites on P-glycoprotein are altered by ATP binding prior to nucleotide hydrolysis. *Biochemistry 39*, 11901−11906.
44. Martin, C., Higgins, C. F., and Callaghan, R. (2001) The vinblastine binding site adopts high- and low-affinity conformations during a transport cycle of P-glycoprotein. *Biochemistry 40*, 15733−15742.
45. Rosenberg, M. F., Velarde, G., Ford, R. C., Martin, C., Berridge, G., Kerr, I. D., Callaghan, R., Schmidlin, A., Wooding, C., Linton, K. J., and Higgins, C. F. (2001) Repacking of the transmembrane domains of P-glycoprotein during the transport ATPase cycle. *EMBO J. 20*, 5615−5625.
46. Callaghan, R., Ford, R. C., and Kerr, I. D. (2006) The translocation mechanism of P-glycoprotein. *FEBS Lett. 580*, 1056−1063.
47. Rosenberg, M. F., Callaghan, R., Modok, S., Higgins, C. F., and Ford, R. C. (2005) Three-dimensional structure of P-glycoprotein: The transmembrane regions adopt an asymmetric configuration in the nucleotide-bound state. *J. Biol. Chem. 280*, 2857−2862.
48. Druley, T. E., Stein, W. D., and Roninson, I. B. (2001) Analysis of MDR1 P-glycoprotein conformational changes in permeabilized cells using differential immunoreactivity. *Biochemistry 40*, 4312−4322.
49. Oloo, E. O., and Tieleman, D. P. (2004) Conformational transitions induced by the binding of MgATP to the vitamin B-12 ATP-binding cassette (ABC) transporter BtuCD. *J. Biol. Chem. 279*, 45013−45019.
50. Zaitseva, J., Jenewein, S., Jumpertz, T., Holland, I. B., and Schmitt, L. (2005) H662 is the linchpin of ATP hydrolysis in the nucleotide-binding domain of the ABC transporter HlyB. *EMBO J. 24*, 1901−1910.
51. Lu, G., Westbrooks, J. M., Davidson, A. L., and Chen, J. (2005) ATP hydrolysis is required to reset the ATP-binding cassette dimer into the resting-state conformation. *Proc. Natl. Acad. Sci. U.S.A. 102*, 17969−17974.
52. Dawson, R. J. P., and Locher, K. P. (2006) Structure of a bacterial multidrug ABC transporter. *Nature 443*, 180−185.
53. Schuldiner, S. (2006) Structural biology: The ins and outs of drug transport. *Nature 443*, 156−157.
54. Aanismaa, P., and Seelig, A. (2007) P-glycoprotein kinetics measured in plasma membrane vesicles and living cells. *Biochemistry 46*, 3394−3404.

BI701385T